JOURNAL OF
Materials
CHEMISTRY

Simultaneous electrodeposition of Cu–In–Se–Te thin films

R. Díaz,[a] G. San Vicente,[b] J. M. Merino,[a] F. Rueda,[a] P. Ocon[b] and P. Herrasti[b]

[a]*Departamento de Fisica Aplicada, Universidad Autonoma de Madrid, 28049 Madrid, Spain*
[b]*Departamento de Quimica-Fisica Aplicada, Universidad Autonoma de Madrid, 28049 Madrid, Spain*

Received 10th February 2000, Accepted 7th April 2000
Published on the Web 8th June 2000

Cu–In–Se–Te thin films have been produced by electrodeposition on molybdenum electrodes supported on glass substrates. The composition of the films is a function of the growth conditions. The best conditions for a near-stoichiometric composition are a deposition potential of −0.5 V *vs.* SCE and a time greater than 4000 s. After electrodeposition the samples are amorphous. However, crystallization of the films can be achieved by various thermal treatments, for example, annealing in a Te atmosphere at 550 °C for 30 minutes followed by annealing under vacuum at 400 °C for 1 h. This produces crystalline quaternary phases, as confirmed by X-ray diffraction. In order to study the optical properties of the films, some samples were grown on indium tin oxide (ITO) electrodes and annealed at 550 °C for 30 min. The observed absorption coefficients showed two regions corresponding to two energy gaps having values of $E_{g1} = 0.81$ eV and $E_{fg1} = 1.28$ eV. The same films exhibited photoelectrochemical responses with flatband potentials of −0.15 V. All samples exhibited p-type conduction.

Introduction

Thin films of Cu–III–VI_2 chalcopyrites (with III = In, Ga and VI = Se, Te) have recently attracted attention as possible substrates for the fabrication of photovoltaic and optoelectronic devices. For example, copper indium diselenide, $CuInSe_2$, has been shown to be one of the most suitable absorber materials for polycrystalline thin film solar cells.[1–4] Indeed, Hedström *et al.* have described $CuInSe_2$ based cells having energy conversion efficiencies as high as 15.4%.[5] Similarly Contreras *et al.*[6] have reported a total-area device efficiency of 18.8% for $Cu(In,Ga)Se_2$.

Various techniques for thin film fabrication have been used, such as molecular beam epitaxy,[7] flash evaporation,[8] spray pyrolysis,[9] RF sputtering[10] and electrodeposition.[11,12] Quaternary mixed chalcopyrites are of special interest because they offer the possibility of tailoring the reflective index, band gap and lattice parameters *via* the film composition.[13–15] A further advantage of using Cu–In(Se,Te) is that quaternary single phases are always p-type, as previously reported.[16,17]

Several papers have shown that chalcopyrite thin films can be grown by electrodeposition. This technique is low-cost, high yield, and safe. Moreover, with suitable annealing conditions, the quality of the films compares well with other methods.

In the present work we report the one-step electrodeposition of Cu–In–Se–Te films under various growth conditions. The composition, morphology and structure of the films were examined. In order to improve cell performance, and to characterize the effects of annealing, different thermal treatments were carried out.

Experimental

CuInSeTe thin films were electrodeposited on molybdenum-coated glass. The Mo layer was deposited by an e-beam technique. The optimal solution composition was chosen after many experiments. The best plating baths consisted of aqueous solutions of 3×10^{-3} M $CuSO_4$, 6×10^{-3} M $InCl_3$, 5×10^{-3} M H_2SeO_3 and 5×10^{-3} M $TeCl_4$, plus 0.5 M citric acid as a complexing agent. Cu, In, Se and Te were deposited by either potentiostatic or voltammetric mode. The deposition times varied between 100 and 7200 s. The counterelectrode was Pt and the reference half-cell was a saturated calomel electrode (SCE).

The single-phase composition of the films was obtained by thermal treatment of the electrodeposited samples. Annealing was carried out in a silica tube in an electric furnace under three different sets of annealing conditions: 1) in an N_2 atmosphere at 350 °C for 2 h; 2) under the same conditions but with a Te gas atmosphere; 3) at 550 °C for 30 min in a Te gas atmosphere

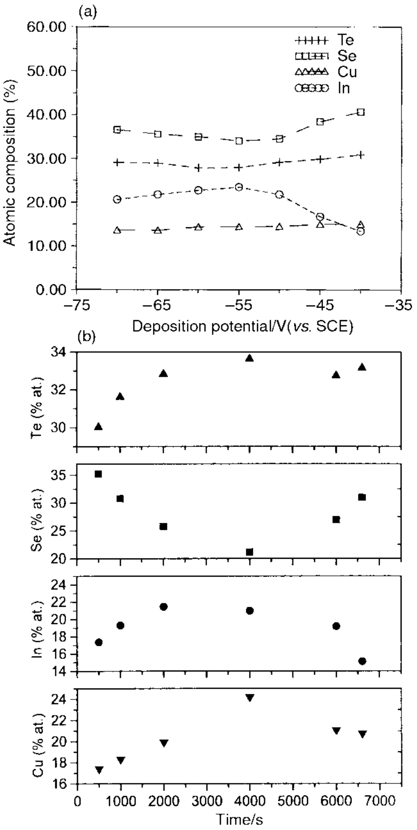

Fig. 1 (a) Composition of the "as grown" films as a function of the applied deposition potential. (b) Composition of the "as grown" films as a function of the deposition time.

DOI: 10.1039/b000168f

Table 1 Composition and growth condition of thin films

Sample	Voltage/V	Time/s	Cu (%at.)	In (%at.)	Se (%at.)	Te (%at.)
A1	−0.4	500	17.84	8.38	42.17	31.6
A2	−0.4	1000	20.19	8.78	37.18	33.86
A3	−0.4	2000	15.02	13.41	40.68	30.88
A4	−0.4	2000	19.07	14.69	30.8	35.44
A5	−0.4	3000	18.7	8.87	38.06	38.06
A6	−0.4	4000	20.79	14.59	29.18	35.44
A7	−0.4	6000	19.32	14.58	29.71	36.39
B1	−0.45	2000	14.99	16.74	38.4	29.87
C1	−0.5	500	17.42	17.36	35.2	30.02
C2	−0.5	1000	18.32	19.32	30.76	31.61
C3	−0.5	2000	14.5	21.79	34.54	29.17
C4	−0.5	2000	19.95	21.46	25.76	32.83
C5	−0.5	4000	24.2	21	21.16	33.63
C6	−0.5	6000	21.09	19.19	26.97	32.75
C7	−0.5	6600	20.76	15.13	30.95	33.16
D1	−0.55	2000	14.49	23.5	34.01	28
D2	−0.55	3000	15.53	23.61	30.72	30.14
D3	−0.55	3600	16.41	24.75	31.85	27
D4	−0.55	5000	18.3	19.74	29.62	32.34
E1	−0.6	500	16.48	19.32	33.15	31.05
E2	−0.6	500	14.73	19.99	37.59	27.69
E3	−0.6	1000	17.37	23.42	29.48	29.73
E4	−0.6	2000	19.76	23.62	24.45	32.17
E5	−0.6	2000	14.41	22.76	34.98	27.85
E6	−0.6	2000	17.4	25.1	20.6	36.91
E7	−0.6	3000	15.89	20.23	28.66	35.21
E8	−0.6	3000	15.5	20.78	36.31	27.41
E9	−0.6	3600	10.2	25.11	39.84	24.85
E10	−0.6	4000	16.76	17.6	28.97	36.67
E11	−0.6	4000	23.11	19.33	22.04	35.53
E12	−0.6	6000	26.33	14.16	19.76	39.75
F1	−0.65	2000	13.64	21.82	35.58	28.96
F2	−0.65	3600	15.39	18.88	33.23	32.5
F3	−0.65	7200	20.88	16.11	26.85	36.16
G1	−0.7	2000	13.69	20.67	36.57	29.07
H1[a]	−0.5	3000	20.49	2.04	16.17	61.29
H2[a]	−0.6	3000	20.48	0.81	14.01	64.70
I1[b]	−0.7–0.4	3000	5.35	20.63	24.4	49.62
I2[b]	−0.7–0.2	3000	15.37	10.00	17.70	56.94
I3[b]	−0.6–0.3	3000	18.32	8.17	17.44	56.08
I4[b]	−0.7–0.4	3000	15.37	11.39	16.17	57.07

[a] Thin film grown with agitation of the bath. [b] Thin film grown with cyclic voltammetry.

followed by 400 °C for 1 h in vacuum. In this latter case the elemental Te was placed close to the electrodeposited films.

The morphology of the films was examined using a Phillips XL30-EDAX PV 9900 scanning electron microscope, and the composition was determined by using an energy dispersive X-ray analyser. Quantitative analysis was achieved by using bulk CuInSeTe as a standard. Structural characterisation of both the as-deposited and annealed films was accomplished by X-ray diffraction using nickel filtered CuK$_{\alpha}$ radiation. Normal incidence transmittance (T) and oblique (39°) reflectance (R) spectra were measured in the 400–2500 nm range using a Cary 17D spectrophotometer. In most cases this allowed us to determine the absorption coefficient, α, for each wavelength, by using a model that takes into account multiple reflections.[18] The electrical properties were obtained by the hot point method.

Results and discussion

Electrodeposition of the films

Different parameters were varied in order to vary the composition of the electrodeposited films. These parameters were: the deposition method, the deposition potential, the deposition time, the solution temperature and the solution composition.

The solution composition was changed while keeping all the other parameters fixed. When the Cu concentration in solution is low, the films are Se rich. Upon increasing the Cu concentration the Se content in the films is reduced. The In/Cu ratio was near to 1 when the Cu concentration was not higher than 3×10^{-3} M. The Te concentration in the bath was increased up to 5×10^{-3}, at Te concentrations lower than this value the formed films have stoichiometric composition; after thermal treatment no Te content was detectable in the films.

In general the method used for deposition was that of constant potential, rather than linearly-varying potential. The latter was not an advance over the constant potential method (the morphology was somewhat more homogenous but the film thickness was less).

Fig. 1a shows the compositions of thin films deposited at constant potential between –0.7 and –0.4 V *vs.* SCE. An increase in the Cu/In atomic ratio is observed as the deposition potential becomes less negative. The Se and Te concentrations are practically constant throughout. At potentials more negative than –0.7 V *vs.* SCE a break in the general behaviour is observed. This effect is probably due to an alteration in the deposition process due to hydrogen evolution. When the potential is more positive than –0.4 V *vs.* SCE indium is not deposited. The best deposition potential for Cu/In = 1 and (Se + Te) near 50% is –0.5 V *vs.* SCE.

Fig. 1b shows element concentrations *versus* deposition times for samples grown at −0.5 V *vs.* SCE. The selenium concentration is high at short times but gradually decreases. The Te concentration is higher than 25% thoughout. Deposition times of at least 4000 s must be used to obtain film thicknesses suitable for solar cell applications (1–2 μm).

Several samples were obtained at the same potential and deposition times, but at different temperatures. This revealed that, at higher temperatures, the adherence of the films was not very good. Above 70 °C the surfaces of the films were so rough that the films easily peeled off the substrates.

Keeping all the other parameters fixed, stirring the solution decreased the concentration of indium but not the concentration of the other elements.

Table 1 shows the growth conditions and compositions of each sample. It is clear that the indium deposition is interfacially controlled and the other components of the film (Se, Te, Cu) are diffusion controlled.

In summary, the best conditions for growing near-stoichiometric quaternary compounds are: constant potential in the range −0.5 and –0.6 V at 20 °C, without stirring the solution, and with deposition times between 3000 and 5000 s.

Morphology and structure of the films

The morphology of the films is generally that of a very high number density of agglomerate granules with diameters of about 0.1 μm, as shown in Fig. 2a. The agglomerates grow to about 2 μm diameter for longer deposition times (4000 s) and the surfaces becomes rougher, Fig. 2b.

"As grown" films on Mo substrates almost always yield amorphous X-ray diffraction patterns: only one (grown at −0.6 V *vs.* SCE) showed a peak ($d = 0.3324$ nm) corresponding to crystalline or possibly a Cu-poor sphalerite phase. As a result, it is generally difficult to identify the chalcopyrite phases.

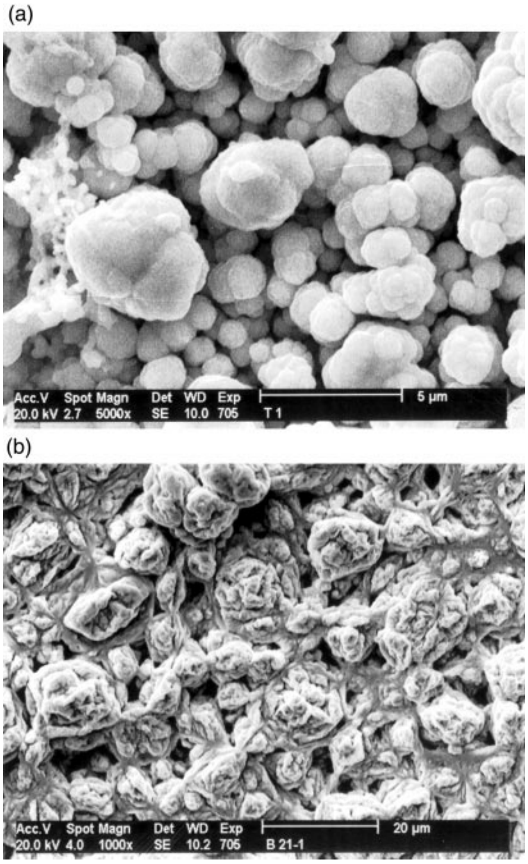

Fig. 2 SEM microphotographs of "as grown" films ($E = -0.6$ V): a) $t = 500$ s, b) $t = 4000$ s.

Table 2 Composition and annealing conditions[a]

Series	Sample	Cu (%at.)	In (%at.)	Se (%at.)	Te (%at.)
A	A3	38.59	20.82	38.64	1.95
A	B1	35.96	24.6	35.67	3.77
A	C3	32.45	28.4	35.93	3.23
A	D1	27.71	32.04	36.57	3.68
A	E5	31.49	32.19	33.89	2.44
A	F1	27.18	35.7	32.95	4.17
A	G1	31.1	33.66	31.78	3.46
B	A1	20.16	7.84	59.42	12.58
B	A2	37.99	12.92	43.72	5.37
B	A4	7.94	17.54	40.63	33.89
B	A6	38.57	22.58	27.66	11.19
B	A7	38.01	21.52	27.17	13.29
B	C1	16.73	16.76	37.01	29.5
B	C2	17.94	19.13	34.22	28.7
B	C4	20.16	22.39	27.17	30.28
B	C5	22.43	22.97	22.39	32.21
B	C6	26.24	23.79	25.95	24.02
B	D2	19.49	27.19	42.03	11.29
B	D4	26.63	28.14	43.94	1.29
B	E1	16.03	17.95	34.52	31.5
B	E4	18.06	23.06	31.7	27.18
B	E8	24.02	29.19	45.16	1.62
B	E11	21.38	24.64	22.95	31.04
B	E12	31.58	31.79	28.74	7.83
B	ITO	15.27	24.94	14.75	45.03
C	C7	20.18	24.92	12.55	42.35
C	D3	9.77	15.98	25.68	48.56
C	E9	13.05	25.93	12.16	48.86
C	F2	12.18	14.22	12.37	61.23
C	F3	20.88	25.45	8.78	44.99
CV	D3	14.92	26.37	7.71	51.01
CV	E9	13.85	25.47	11.52	49.16
CV	F2	15.6	16.38	10.12	57.9
CV	F3	21.83	20.84	10.26	47.07

[a] The thermal treatment is done: Series A: at 350 °C during 2 h in N_2 atmosphere. Series B: at 350 °C during 2 h in still Te atmosphere. Series C: at 550 °C during 30 min in still Te atmosphere. Series CV: at 400 °C during 1 h in vacuum.

Thermal treatment of the films

Composition. Table 2 lists the thermal treatments and the resulting compositions of the films. Annealing in N_2 at 350 °C for 2 h decreased the Te concentration to 4%at. (Series A). For this reason all subsequent treatments were carried out in a Te atmosphere (Series B). Unfortunately, when we studied the X-ray diffractograms of these samples, we found that the films were not quaternary single phases, but rather ternary phases plus elemental Te. We therefore annealed a third series of samples at 550 °C for 30 min in Te atmosphere (Series C). After this treatment the chalcogen content of the films was high. Further annealing at 400 °C in vacuum for 1 h led to changes in film composition (Series CV).

Structure. All thermal treatments produced large increases in the intensity and number of diffraction peaks, indicating crystallization. As mentioned above, the films annealed at 350 °C for 2 h in N_2 exhibited the $CuInSe_2$ chalcopyrite phase plus elemental Te. Chalcopyrite phase has been assumed since this phase was found in bulk and thin film compounds $A^{I}B^{III}C^{VI}$.[11,16,17,19] Annealing in Te atmosphere produced an additional secondary Cu_xTe_y phase and a small peak with $d = 0.3407$ nm and a relative intensity $I = 3.26\%$ that corresponded to the chalcopyrite structure with lattice parameters $c/a = 2$ and $a = 0.590$ nm.

When the annealing temperature was increased to 550 °C, the samples produced two quaternary phases with different lattice parameters. These were due to different Se/Te concentrations in the lattice (Fig. 3a). In an attempt to eliminate the elemental Te , the samples were further annealed at 400 °C in vacuum for 1 h. The X-ray diffractogram shows that the elemental Te disappeared while three quaternary phases appeared (Fig. 3b).

Optical properties

A thin film was electrodeposited on an indium tin oxide (ITO) coated glass substrate. The thickness of the film was about 0.5 μm. It was annealed at 550 °C for 30 min in a Te atmosphere. The film after annealing was a single phase (Fig. 3c) and its composition is shown in Table 2.

Normal incidence transmittance (T) and oblique (39°) reflectance (R) spectra of annealed samples were used to determine the absorption coefficients of the quaternary compounds (Fig. 4). Fig. 5a and 5b show $(\alpha h\nu)^2$ and $(\alpha h\nu)^{2/3}$ as a function of $h\nu$ The energy gaps were determined by the intersections with the $h\nu$ axis. Two transitions were observed corresponding to the direct and second forbidden gaps respectively.[16,20] The second gap was evaluated by subtracting the absorption response of the first.[16,17] The energy gap values, $E_{g1} = 0.81$ eV and $E_{fg1} = 1.28$ eV, corresponded to the known quaternary phase.[16,20] In addition p-type conduction was found in all annealed samples.

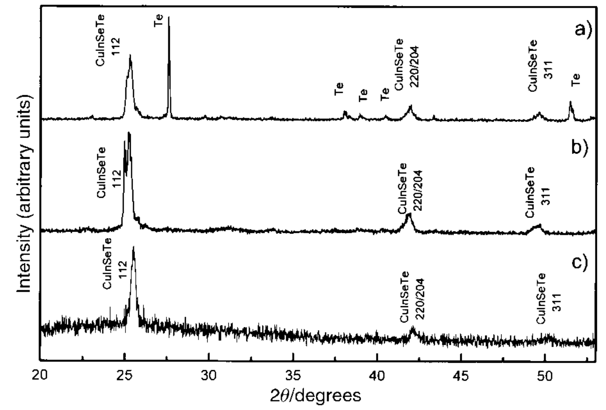

Fig. 3 X-Ray diffractograms of CuInSeTe films: a) on a substrate after annealing at 550 °C in N_2+Te atmosphere, and b) same as a) after annealing at 400 °C in vacuum and c) on ITO substrate after annealing at 550 °C in N_2+Te atmosphere.

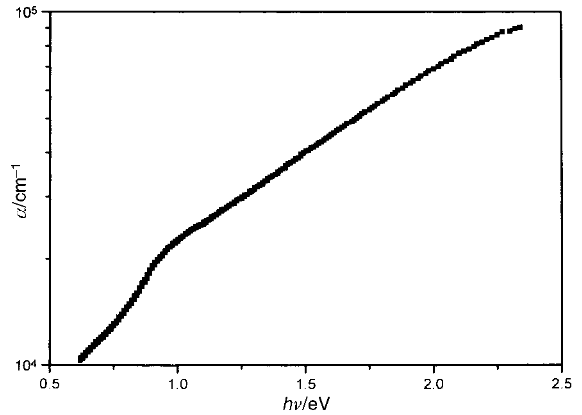

Fig. 4 Absorption coefficients (α) for Cu–In–Se–Te annealed film (on ITO, $V = -0.7$ V, $t = 200$ s).

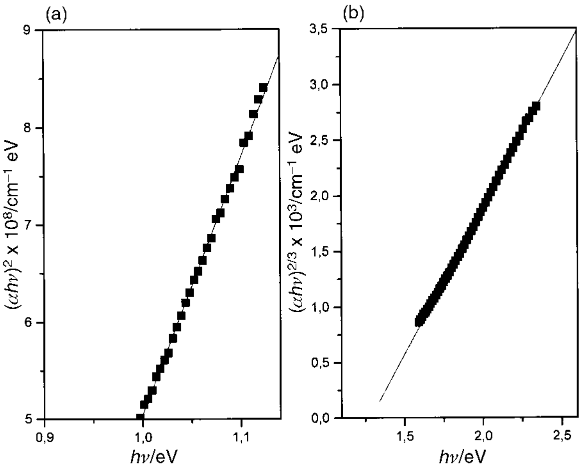

Fig. 5 Fit of energy gaps for a sample on ITO after annealing: a) fit of first gap and b) fit of forbidden gap.

Morphology

Fig. 6 shows SEM micrographs of the surfaces of two films grown at –0.5 V *versus* SCE and annealed at 350 °C either in N_2 or Te atmospheres. Annealing in N_2 results in a very high number density of large and small globules. Annealing in Te leads to a collapse of globular grains across the sample. If the temperature is increased large faceted crystallites are formed.

Photoelectrochemistry of the films

Photoelectrochemistry of electrodeposited CuInSeTe films was studied in 0.5 M Na_2SO_4 solution. We studied the photoelectrochemical properties to confirm their photovoltaic activity. A typical *I–V* curve obtained while sweeping the cell voltage under chopped polychromatic illumination is shown in Fig. 7. Some differences in the photoresponse were observed depending on the direction of the potential sweep. The hysteresis between anodic and cathodic sweeps may be explained by oxidation or reduction of surfaces species, or by band edge shifts at the semiconductor–solution interface. Towards more negative potentials the photocurrent amplitude increases considerably due to the reduction of protons by photogenerated electrons. At positive potentials, the photocurrent and an oxidation process occur simultaneously. Photocurrent–time transients were used to determine the flatband potential, V_{fb}, of the semiconductor material in 0.5 M Na_2SO_4 solution. (V_{fb} is

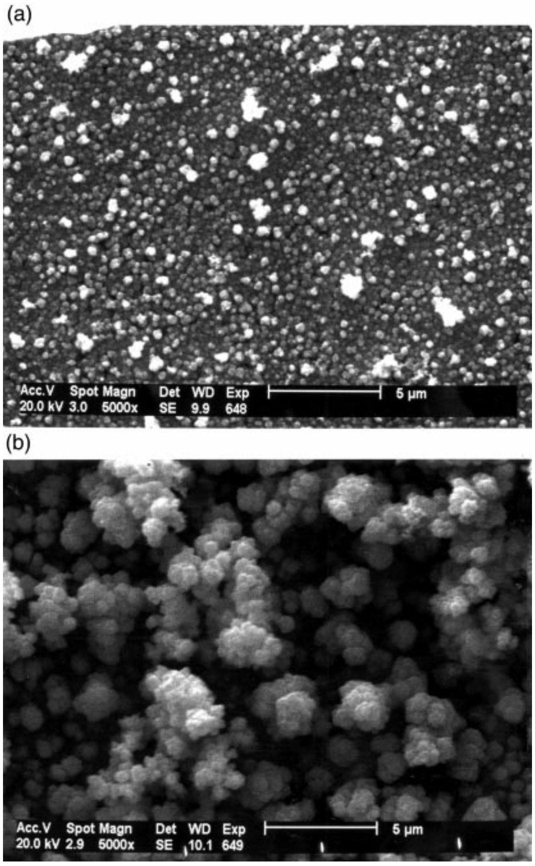

Fig. 6 SEM microphotographs of annealed films: a) in air, 350 °C, 0.5 h; b) in still N_2+Te, 350 °C, 1 h.

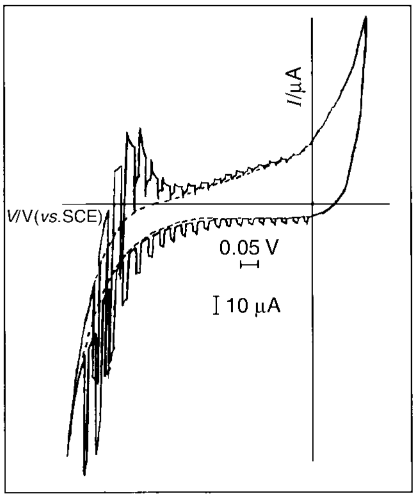

Fig. 7 *I–V* curve taken for "as grown" film in 0.5 M Na_2SO_4 solution under chopped tungsten lamp illumination.

usually close to where the stationary photocurrent goes to zero or changes sign). The V_{fb} value is –0.15 V *versus* SCE in Na_2SO_4. When the electrodes are first illuminated with polychromatic light, an initial cathodic photocurrent spike is observed, but after a few seconds a stationary cathodic photocurrent develops. When the illumination is switched off, the current returns to its initial level. The ratios between initial and stationary photocurrents begin to decrease when the polarization potential is changed to more negative values. This is attributed to the appearance of a reduction reaction that competes with the photooxidation of the redox couple in solution.

Conclusions

Cu–In–Se–Te compounds have been grown by electrodeposition on molybdenum substrates. The resulting films are amorphous and have compositions which vary with deposition conditions. The same films show photovoltaic activity and p-type conduction. Interestingly, the crystallinity of the films is improved by thermal treatment. Indeed, samples annealed sequentially in Te atmosphere and vacuum produce well-defined quaternary phases. The film formed on ITO has a direct energy gap of 0.81 eV.

Acknowledgements

The financial support of the Spanish Government through the C.I.C.Y.T. (Project No. ESP96-0504) is gratefully acknowledged.

References

1 H. W. Schock, *10th Eur. Photov. Sol. Ener. Conf.*, Kluwer Academic Publishers, London, 1991, p. 777.
2 L. Thouin and J. Vedel, *J. Electrochem. Soc.*, 1995, **142**, 2996.
3 J. Herrero and C. Guillen, *J. Appl. Phys.*, 1991, **69**, 429.
4 F. Guillemoles, P. Cowache, S. Massacceri, L. Thouin, S. Sanchez, D. Lincot and J. Vedel, *Adv. Mater.*, 1994, **6**, 379.
5 J. Hedstrom, H. Olsen, M. Bodegard, A. Kylner, L. Stolt, O. Harikim, M. Ruckh and H. W. Schock, *Proc. 23rd IEEE Photovoltaic Spec. Conf. Louisville*, IEEE, New York, 1993, p. 364.
6 M. A. Contreras, B. Egaas, K. Ramanathan, F. Hasoon and R. Noufi, *Proc. E-MRS 1999 Spring Meeting (Strasbourg, 1999)*.
7 S. Kohiki, M. Nishitani, K. Nishikura, T. Negami, M. Terauchi and T. Hirao, *Thin Solid Films*, 1992, **207**, 265.
8 V. Canevari, N. Romeo, G. Sberveglieri, L. Zanotti and M. Curti, *Mater. Chem. Phys.*, 1983, **9**, 205.
9 K. Subbaramaiah and V. Sundara Raja, *J. Mater. Sci. Lett.*, 1992, **10**, 1344.
10 J. A. Thornton, T. C. Lommasson, H. Talich and B. H. Teseng, *Sol. Cells*, 1988, **24**, 1.
11 C. Guillén and J. Herrero, *J. Electrochem. Soc.*, 1994, **141**, 226.
12 Y. Sudo, S. Endo and T. Irie, *J. Appl. Phys.*, 1993, **32**, 1562; J. Vedel, *Adv. Mater.*, 1994, **6**, 379.
13 L. L. Kazmerski, M. Hallerdt, P. J. Ireland, R. A. Mickelson and W. S. Chen, *J. Vac. Sci. Technol. A*, 1983, **1**, 395.
14 J. Sewchun, J. Loferski, D. Burk, B. K. Garside, R. Baulieu and D. Polk, *Conf. Rec. 14th IEEE Photovoltaic. Spec. Conf.*, IEEE, New York, 1980, p. 650.
15 M. Quintero and J. C. Wooley, *J. Appl. Phys.*, 1984, **55**, 15.
16 R. Diaz, M. León and F. Rueda, *Jpn. J. Appl. Phys.*, 1992, **31**, 3675.
17 R. Diaz, M. León and F. Rueda, *J. Vac. Sci. Technol. A*, 1992, **10**(2), 295.
18 E. Elizalde and F. Rueda, *Thin Solid Films*, 1984, **122**, 45.
19 J. M. Merino, J. L. Martín de Vidales, S. Mahanty, R. Diaz, F. Rueda and M. Leòn, *J. Appl. Phys.*, 1996, **80**(7), 5610.
20 T. Tinoco, M. Quintero and C. Rincón, *Phys. Rev. B*, 1991, **44**(4), 1613.